



A Simulation for Growth Evaluation of Multiple Small Cracks

Masayuki Kamaya ¹⁾, Takayuki Kitamura ²⁾

¹⁾ Institute of Nuclear Safety System, Inc. (INSS), Fukui, Japan

²⁾ Kyoto University, Kyoto, Japan

ABSTRACT

It is important to understand the behavior of small cracks, which are initiated in the components of nuclear power plants, in terms of high reliability. However, it is difficult to predict the growth behavior, because the growth rates of small cracks are unsteady due to the microstructural inhomogeneity of polycrystalline. Furthermore, in corrosive environments, multiple small cracks are initiated and mutually affect in the growth process. In this study, a Monte Carlo simulation is developed in order to analyze the random behavior. The unsteady growth of small cracks is simulated considering the influences of interaction between multiple cracks and microstructure on the stress intensity factor, which governs the crack growth rates. The simulation focuses on primary water stress corrosion cracking (PWSCC) of mill-annealed alloy 600. The crack size distributions obtained by the simulation agree well with the experimental results. The maximum crack size is statistically estimated by the simulation.

KEY WORDS: small crack, multiple crack, Monte Carlo simulation, microstructure, crack growth, lifetime prediction.

INTRODUCTION

As the initiation and growth of small crack governs the life of components [1], it is important to understand the growth behavior in order to maintain the high reliability of nuclear power plants. However, the unsteady growth behavior brings about difficulty in the prediction of component lifetime. Averaging the anisotropy of each crystal, the macroscopic behavior of polycrystalline materials is isotropic and homogeneous in terms of elastic deformation. However, the anisotropic and inhomogeneous property influences on the stress field around a crack if the crack size is small in comparison with the grain, and causes unsteady crack growth [2] (hereafter “polycrystal effect”). The second factor is the influence of crack kinks caused by grain boundaries (hereafter “crack kink effect”). Third factor, which causes unsteady behavior in the stress corrosion cracking (SCC), is the interaction between multiple cracks [3] (hereafter “interaction effect”). In SCC, many cracks are initiated and mutually affect each other [4]. The unsteady growth behavior of small cracks stems on the factors, and there is no reliable method for predicting probabilistic lifetime proposed.

In the present study, a Monte Carlo simulation model is developed for the unsteady small crack growth behavior by considering the influences of the interaction effect, polycrystal effect and crack kink effect.

EXPERIMENTAL OBSERVATION

Experiments of primary water stress corrosion cracking (PWSCC) were conducted in a previous study [5]. This paper briefly summarizes them.

Experimental method

The material used for the study was alloy 600, which is mill-annealed at 1253 K. This was produced under almost the same procedure as the one used in the head penetrations of reactor pressure vessels. It was cut into plane specimens of 75 mm long with a gage length of 20 mm and 2x4 mm cross section. The specimens were polished with #1200 emery paper before the SCC experiment. 11 specimens were subjected to constant tensile load of 529 MPa under a simulated PWR primary environment (500 ppmB, 2 ppmLi, 4 ppmH₂, < 5 ppb O₂) at 633 K. All the tests were carried out in an autoclave, which was directly connected to a recirculation test loop. In order to investigate the relationship of crack extension and exposure time, specimens were taken out at specific times, 500 h, 1000 h, 1500 h and time to fracture (TTF). The precise crack size, which is deeper than 3 μm, was measured by means of an optical microscope after polishing and etching the cross section.

Experimental results

Many intergranular cracks were observed at the cross sections. The number of cracks and the maximum crack depth is plotted against the exposure time in Figs.1 and 2, respectively. The number as well as the size increased as the time passed.

It is possible to estimate the growth rate of the maximum crack (da_{\max}/dt) by the gradient of the interpolated curve in Fig.2. The growth rates are plotted against the stress intensity factor K in Fig.3, when the K values were calculated assuming a semi-circular crack in an infinite plate [6]. The relationship obtained by the least squares method is formulated as

$$\frac{da_{\max}}{dt} = 5.24 \times 10^{-14} K^{3.46} . \quad (1)$$

The growth rate is in m/sec and K value in $\text{MPa}\sqrt{\text{m}}$. The $da/dt - K$ relation of macrocrack in PWCC of alloy 600 obtained by several researchers are also shown in Fig.3 [7][8]. The relationship, Eq.(1), coincides fairly well with the macroscopic crack growth behavior obtained by the compact tension specimen [7].

In this study, grain boundaries (GBs) along the crack path are classified into two categories: crack-initiated GB and crack-propagated one. The inclinations of the GBs with respect to the stress direction are investigated, respectively where θ_i and θ_p are defined in Fig.4. Observed crack inclination angle profiles are summarized in Fig.5. The low proportion in the high angle region indicates that the applied stress is predominant for the cracking behavior.

SIMULATION PROCEDURE

This simulation focuses on the initiation and growth behavior of multiple surface cracks observed in the experiments, and consists of three parts, preparation of the material (Step 1), crack initiation (Step 2) and crack propagation (Step 3), as shown in Fig.6.

The material is assumed to mill-annealed alloy 600, which is isotropic polycrystal of 20~60 μm in diameter. Using the observation data of material, the parameters, which statistically reproduce the microstructure, are determined in Step 1 in advance.

In Step 2, cracks are created so that the relationship between the number of cracks and time agrees with the experimental result as shown in Fig.1. 68 crack initiation per 1000 h on the 1x1 mm plane gives fairly good agreement in the number of cracks on the cross section, except the data of TTF, as shown in Fig.7.

The initiated cracks propagate in Step 3. The extension length at each step is calculated using K value based on the relation expressed in Eq. (1). Under a fixed stress, the stress intensity factor K is depending not only on the crack size and the shape but also on the crack kink, the interaction between neighboring cracks, anisotropy of each crystal. Their effect is eminent in the propagation of small crack. The K value is therefore expressed by:

$$K = C_o F_{\text{mut}} F_{\text{ani}} F_{\text{kink}} \sigma_o \sqrt{\pi a} , \quad (2)$$

where F_{mut} , F_{ani} and F_{kink} , present the effects, respectively. C_o is a constant, a is crack size and σ_o (=529 MPa in the following case) is applied stress. In addition, each GB possesses their own resistance against the cracking due to the microstructure, i.e. carbide precipitation, which is represented by a random variable, Z_p . Summarizing these factors, the crack extension length Δa is calculated by:

$$\Delta a = D_o Z_p \left(F_{\text{mut}} F_{\text{ani}} F_{\text{kink}} \sigma_o \sqrt{\pi a} \right)^{m_p} \Delta t , \quad (3)$$

where D_o is a constant and Δt is the interval of the step which is controlled so that the Δa does not exceed 5% of crack length a in the simulation. Cracks are assumed to maintain the semi-circular shape. As described later, each crack has two F_{mut} value derived at surface points in every step, although the Z_p , F_{ani} and F_{kink} is assigned one value depending on crack size. Then, the extension length in depth direction is set as half of the surface extension length $\Delta a_{(\text{Left})}$ and $\Delta a_{(\text{Right})}$ as shown in Fig.8. Steps 2 and 3 are repeated until integration of Δt reaches 1500 h.

Since each GB possesses their own resistance, the crack faces various resistances along the crack front. Then, the Z_p is given by following equation using the number of GBs existing along the front, N_g :

$$Z_p = \frac{\sum_{n=1}^{N_g} z^{(n)}}{N_g} , \quad (4)$$

where $z^{(n)}$ is the resistance factor assigned to each of GBs as shown in Fig.8, and determined by a random number in the range $0 \leq z \leq 1$. N_g is determined by the length of crack front and average grain diameter [2]. According to this equation, Z_p decreases as the crack size increases and becomes 0.5 for the macroscopic crack.

Similarly, the effects of crack kink are different at each GB depending on the deflection angle. The relationship between the deflection angle, α , and change in K values was investigated in a previous study [2]. It was revealed that the K values of

the kinked crack are approximated by the following equation, regardless of the complex intergranular crack configuration:

$$\frac{k_1}{K_1} = \cos^3\left(\frac{\alpha}{2}\right), \quad (5)$$

where k_1 is the K value of mode I at a kinked crack tip and K_1 is the K value of a crack without kink. Then, the crack kink effect, F_{kink} , is determined by the following equation:

$$F_{\text{kink}} = \frac{\sum_{n=1}^{N_g} \cos^3\left(\frac{\alpha^{(n)}}{2}\right)}{N_g}, \quad (6)$$

where $\alpha^{(n)}$ means the crack kink angle at crack front, and is given by random numbers following Fig.5. The F_{kink} converges to 0.917 when the crack size increases.

As for the polycrystal effect, F_{ani} , of the semi-circular surface crack, the previous study [2] revealed that the distribution of K values due to the polycrystal effect (anisotropy of each crystal) statistically obeys a normal distribution and that the standard deviation decreases as the crack size increases, as shown in Fig.9. The mean value is an almost constant value, 0.707. In the simulation, the F_{ani} is determined by random numbers of the normal distribution shown in Fig.9.

The interaction effect between multiple cracks is evaluated by the Body Force Method (BFM), which is effective for calculating the K value of cracks that mutually affect each other. Here, the cracks are assumed to be through ones for simplicity. The interaction effect, F_{mut} , is defined using the K value obtained by the BFM, $K_{(\text{BFM})}$, as follows:

$$F_{\text{mut}} = \frac{K_{(\text{BFM})}}{\sigma_o \sqrt{\pi a}} \quad (7)$$

F_{mut} equals 1 provided there is no interaction.

Although the F_{mut} is calculated at each step, the Z_p , F_{ani} and F_{kink} is not always renewed. These values are assigned for projected crack paths determined for each crack as shown in Fig.10. The projected path is evaluated from GBs, which lengths and inclinations are determined from the length distribution of the test material and crack inclination angle distribution shown in Fig.5, respectively. The average grain boundary length is 11 μm . The first path from the center is assumed to be equivalent to the crack initiation size.

The constant parameters are set to $D_o=1.12 \times 10^{-13}$ and $m_p=3.46$, so that the growth rate of macroscopic cracks ($Z_p=0.5$, $F_{\text{mut}}=1$, $F_{\text{ani}}=0.707$, $F_{\text{kink}}=0.917$) agrees with Eq.(1). The growth rate of macroscopic cracks can be derived as follows:

$$\frac{da}{dt} = 1.37 \times 10^{-14} \left(\sigma_o \sqrt{\pi a} \right)^{3.46} \quad (8)$$

The growth rate is given in m/sec, $\sigma_o(=529\text{MPa})$ in MPa and a in m. The simulation is carried out 100 times for statistical analyses.

SIMULATION RESULTS

Figure 11 shows the simulated behavior of crack initiation and growth on the plane and on the cross section. In this figure, the multiple cracks are expressed by perpendicular lines to the stress direction for simplicity. Some cracks mutually affect each other as cracks • and •. The change in crack size is plotted in Fig.12 for numbered cracks. Cracks • and • grow with fast rate while cracks • and • become dormant.

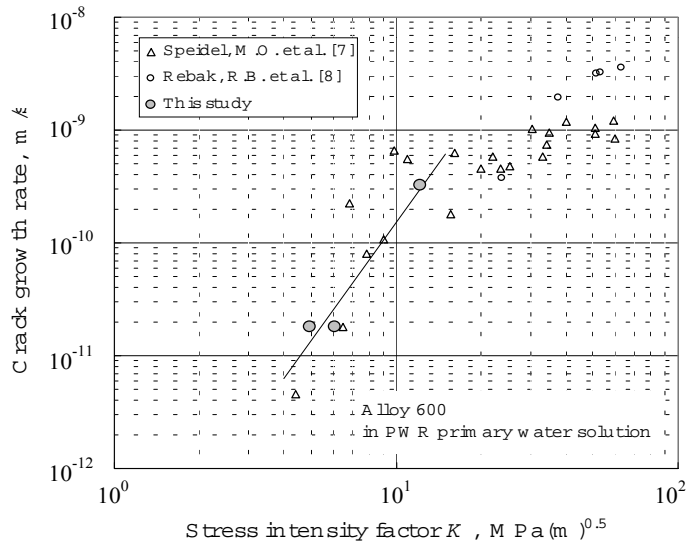
The crack depth distribution at the cross section at 1500 h is shown in Fig.13 together with the experimental results. As it shows good agreement the simulation is statistically valid.

The relationship between the crack size and crack growth rate is shown in Fig.14. The crack growth rate shows eminent scatter when the size is smaller than 20 μm . The variation decreases as the crack size increases and converges to the macroscopic crack growth rate, which is expressed by Eq.(8) and is shown by the solid line in Fig.14.

The Gumbel probability plot for the crack sizes, which are the maximum ones at the end of each simulation (hereafter, main crack), is shown in Fig.15. The figure points out that the size of main crack is reasonably predicted by the obtained Gumbel distribution. By taking the fixed value of $Z_p=0.5$, $F_{\text{ani}}=0.707$ and $F_{\text{kink}}=0.917$, the simulation imitated the macroscopic crack growth behavior and results are also plotted in Fig.15. These sizes are smaller than those of the previous simulation. It is because that the growth rate of main cracks tends to be faster than that of the macroscopic crack as shown in Fig.14. This implies that, in the prediction of small cracks, we have to take the microstructural effect such as the effects of polycrystal, kink and interaction for a conservative evaluation.

CONCLUSION

1. In this study, a Monte Carlo simulation model is developed for reproduce of small crack growth behavior by



considering Wang, Y.Z., Atkinson, J.D., Akid, R. and Parkins, R.N., “Crack Interaction, Coalescence and Mixed Mode Failure Mechanics”, *Fatigue Fract. Engng Mater. Struct.*, 19, 1996, pp. 427-439.

2. Kamaya, M. and Totsuka, N., “Influence of Interaction between Multiple Cracks on Stress Corrosion Crack Propagation”, *Corrosion Science*, 44, 2002, pp. 2333-2352
3. Newman, J.C. and Raju, I.S., “An Empirical Stress-Intensity Factor Equation for the Surface Crack”, *Engng Fract. Mech.*, 15, 1981, pp. 185-192.
4. Speidel, M.O. and Magdowski, R., “Stress Corrosion Crack Growth in Alloy 600 Exposed to PWR and BWR Environments”, *Proc. CORROSION/2000*, paper no.222, Orlando, U.S.A. March 2000.
5. Rebak, R.B, McIlree, A.R. and Szklarska-Smialowska, Z., “Effect of pH and Stress Intensity on Crack Growth Rate in Alloy 600 in Lithiated + Borated Water at High Temperatures”, *Proc. 5th Int. Symposium on Environmental Degradation of Materials in Nuclear Power System – Water Reactors*, pp. 511-517, Monterey, U.S.A., August 1991.

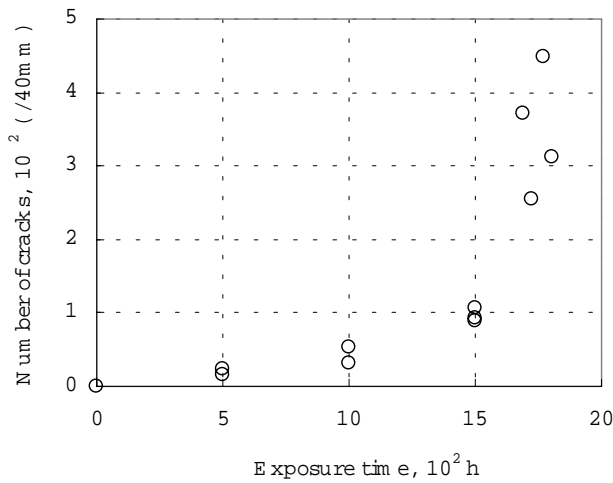


Fig.1 Change in number of cracks at cross-section with exposure time.

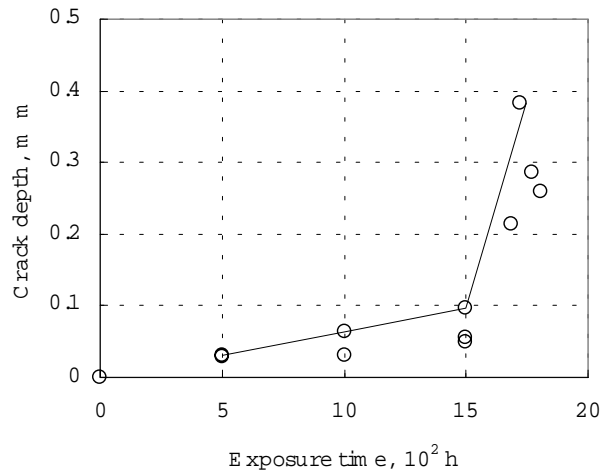


Fig.2 Change in maximum crack depth on a cross-section with exposure time.